J. Fluid Mech. (1975), *vol.* 71, *part* 1, *pp.* 89–104
Printed in Great Britain

Wave propagation in a stratified shear flow

By R. J. HARTMAN
Department of Physics, University of California, Santa Barbara

(Received 6 August 1973 and in revised form 16 November 1974)

The linearized initial-value problem for a two-dimensional, unbounded, exponentially stratified, plane Couette flow is considered. The solution is used to evaluate the evolution of wave-packet perturbations to the mean flow for all Richardson numbers $J > \frac{1}{4}$, demonstrating that a consistent wave-packet approach to wave propagation in these flows is possible for all $J > \frac{1}{4}$. It is found that the vertical influence of a wave-packet perturbation is limited to a distance of order $(J-\frac{1}{4})^{\frac{1}{2}}/k_0$, where k_0 is the magnitude of the initial central wave vector. These results are used to clarify the $J \gtrsim \frac{1}{4}$ conclusions of an earlier treatment by Booker & Bretherton.

1. Introduction

The first detailed attempt to solve the initial-value problem for a stratified shear flow seems to have been that of Eliassen, Høiland & Riis (1953). That theirs is not the *complete* solution to the problem for the stable regime (Richardson number $J > \frac{1}{4}$) was demonstrated by Case (1960) and Dyson (1960), who, though apparently unaware of the earlier work, showed that the discrete normal modes of the kind considered by Eliassen *et al.* for $J > \frac{1}{4}$ do not constitute a mathematically complete set of functions. The Fourier and Laplace inversion integrals which formally complete the initial-value problem of Case appear to be too involved for computation of the time evolution of any interesting initial disturbances. Case was, however, able to give a rather thorough stability analysis for the problem of a semi-infinite exponential atmosphere.

Bretherton (1966) and Booker & Bretherton (1967) considered the problem of wave propagation in a stratified shear flow with specific attention to critical-level absorption of wave energy and momentum. Bretherton (1966) used a WKB approximation to the governing equations valid for large Richardson numbers ($J \gg 1$). Booker & Bretherton (1967) considered first a single normal-mode solution, and associated the discontinuity in normal-mode amplitude $\exp[-\pi(J-\frac{1}{4})^{\frac{1}{2}}]$ at the critical level with a 'transmission coefficient' for wave energy and momentum. They then considered the specific initial/boundary-value problem of flow over an abruptly imposed sinusoidal corrugation in an attempt to demonstrate the validity of their interpretation of the normal-mode discontinuity.

In this paper we present, for an unbounded fluid, a formal solution to the initial-value problem of Eliassen *et al.*, Case and Dyson which is sufficiently simple that the evolution of realistic disturbances may be evaluated directly. This solution is then used to discuss the problem of wave-packet propagation and absorption considered by Bretherton (1966) and Booker & Bretherton (1967). In particular we consider the evolution of initial wave-packet perturbations to the flow, giving specific attention to their trajectories and energetics. It is demonstrated that the problem of internal wave-packet propagation in the presence of uniform shear, regardless of its strength, is analogous to that in an intuitively simpler system, namely an unsheared flow with a time-dependent buoyancy (Brunt–Väisälä) frequency.

The assertion sometimes made (see, for example, Booker & Bretherton 1967) that a consistent wave-packet approach to wave propagation in these flows is restricted to arbitrarily large J is shown to be incorrect. A well-defined (physical and mathematical) picture of wave-packet propagation that is completely consistent for all $J > \frac{1}{4}$ is presented. The specific computation of wave-group propagation and absorption in the regime $J \gtrsim \frac{1}{4}$ serves to supplement and clarify the earlier conclusions of Booker & Bretherton (1967) based on the normal-mode discontinuity.

The approach taken here is free from ambiguities arising from the mathematical singularity at a normal-mode critical level. In particular, it is not necessary to appeal to the effects of finite viscosity and thermal conductivity for a formal verification of the validity of the mathematical approach (see Hazel 1967). The procedure outlined herein also copes readily with wave propagation in more complex basic systems.

Although our approach is, strictly speaking, limited to a linear (Couette) velocity profile, it may be extended via a WKB-type procedure to more general problems where the shear and buoyancy frequencies vary sufficiently slowly with height. Also, discontinuities in flow parameters may be easily dealt with.

2. The governing equations

We choose as our basic model a two-dimensional, unbounded, plane Couette flow with exponential stratification. The equilibrium velocity, pressure and density are given by

$$\mathbf{V}_0 = U_0(z)\,\hat{\mathbf{x}} = Rz\hat{\mathbf{x}}, \tag{2.1}$$

$$dP_0(z)/dz = -\rho_0(z)\,g, \tag{2.2}$$

$$\rho_0(z) = \rho_{00}\exp\left(-z/H_\rho\right), \tag{2.3}$$

where g is the acceleration due to gravity, ρ_{00} is a mean density and H_ρ is the scale height for the variation of density. Here and elsewhere, a caret denotes a unit vector. We assume an incompressible fluid, which permits the definition of a stream function $\boldsymbol{\psi} = \psi\hat{\mathbf{y}}$ through

$$\mathbf{v} = \nabla\times\boldsymbol{\psi} = (-\partial\psi/\partial z, \partial\psi/\partial x). \tag{2.4}$$

The vorticity $\boldsymbol{\zeta}$ is given by

$$\boldsymbol{\zeta} = \zeta\hat{\mathbf{y}} = \nabla\times\mathbf{v} = -\nabla^2\boldsymbol{\psi}. \tag{2.5}$$

Defining a (constant) squared buoyancy frequency

$$N^2 \equiv -\frac{g}{\rho_0}\frac{d\rho_0}{dz} = \frac{g}{H_\rho},$$

the (linearized) Boussinesq equation of motion is

$$\left(\frac{\partial}{\partial t}+Rz\frac{\partial}{\partial x}\right)^2 \nabla^2\psi + N^2\frac{\partial^2\psi}{\partial x^2} = 0. \tag{2.6}$$

Here and below, all quantities refer to deviations from equilibrium.

For our simple model, analysis is greatly facilitated by a transformation to co-ordinates convecting with the mean flow. The transformation defined by

$$\xi = x - Rzt, \quad \eta = z, \quad \tau = t \tag{2.7}$$

leads to a governing equation of the form

$$\left\{\frac{\partial^2}{\partial\tau^2}\left[\frac{\partial^2}{\partial\xi^2}+\left(\frac{\partial}{\partial\eta}-R\tau\frac{\partial}{\partial\xi}\right)^2\right]+N^2\frac{\partial^2}{\partial\xi^2}\right\}\psi(\boldsymbol{\xi},\tau) = 0, \tag{2.8}$$

which evidently permits Fourier decomposition in the 'spatial' co-ordinates $\boldsymbol{\xi} = (\xi, \eta)$. In preparation for this decomposition, we define a dimensionless time variable by

$$T(\mathbf{k}) = Rt - k_2/k_1 = R\tau - k_2/k_1, \tag{2.9}$$

where $\mathbf{k} = (k_1, k_2)$ is the wave vector of a particular Fourier component.† In the following, we shall have occasion to take advantage of a simple relationship between the Fourier transforms of the stream function ψ and the vorticity ζ. In view of (2.5), (2.7) and (2.9), we have

$$\tilde{\zeta}(\mathbf{k}, T) = k_1^2(1+T^2)\,\tilde{\psi}(\mathbf{k}, T), \tag{2.10}$$

where $\tilde{\zeta}(\mathbf{k}, T)$, etc., denote the Fourier-transformed quantities.

In view of (2.9) and (2.10), the Fourier transform of (2.8) may now be conveniently written as

$$\frac{d^2\tilde{\zeta}(\mathbf{k}, T)}{dT^2} + \frac{J}{1+T^2}\tilde{\zeta}(\mathbf{k}, T) = 0, \tag{2.11}$$

where

$$J \equiv N^2/R^2 \tag{2.12}$$

is the Richardson number, everywhere constant in this model. The convected co-ordinate scheme, and in particular (2.11) have been previously used by Phillips (1966) in a WKB approximation to obtain a proposed spectrum for internal waves in a weakly sheared thermocline.

The formal solution to the initial-value problem defined by our model system plus an arbitrary initial disturbance (taken for convenience to be given by $\zeta(\mathbf{x}, t=0)$, $\dot{\zeta}(\mathbf{x}, t=0)$) is now simply given by

$$\zeta(\boldsymbol{\xi}, \tau) = \frac{1}{(2\pi)^2}\int_{-\infty}^{\infty}\int_{-\infty}^{\infty} e^{i\mathbf{k}.\boldsymbol{\xi}} \quad \tilde{\zeta}(\mathbf{k}, \tau)\,dk_1\,dk_2, \tag{2.13}$$

† In convected co-ordinates the wave vector $\mathbf{k}$ of a particular Fourier component is constant in time while in unconvected ('laboratory') co-ordinates the wave vector $\boldsymbol{\kappa}(t)$ rotates clockwise from its initial value $\boldsymbol{\kappa}(t=0) \equiv \mathbf{k}$ and increases in magnitude according to $\tan\theta_\kappa = k_2/k_1 - Rt \equiv -T(\mathbf{k}, t)$, $\kappa^2(t) = k_1^2(1+T^2)$, where θ_κ is the instantaneous polar angle of the wave vector, measured from the horizontal. See figure 2.

where $\tilde{\zeta}(\mathbf{k},\tau)$ is the solution to (2.11) corresponding to the appropriate initial conditions. We henceforth deal primarily with the vorticity ζ for convenience. The stream function (and hence the velocities) follows from a similar expression according to (2.10).

It is evident from the result (2.11) that the initial-value problem for a single Fourier component in an unbounded shear flow, when expressed in convected co-ordinates, is completely analogous to the initial-value problem in the absence of shear but with, in the most general situation, a time-dependent buoyancy parameter $N^2(t)$. The physical situation is indicated in the footnote on p. 91 (see also figure 2). It is important to appreciate that the effect of the imposed shear is to carry the planes of constant phase of an initial plane wave disturbance as if they were fixed in the fluid. A purely kinematic approach using this fact alone, along with the familiar zero-shear result that the time dependence of a plane wave disturbance is $\exp(iNt\cos\theta_\kappa)$, i.e. it depends only on the direction of the wave vector, reproduces the most important physical features (for $J > 1$) of the exact treatment given in § 3 (Hartman 1973).

3. General solutions

Before giving the general solutions to (2.11), it is worthwhile to note their asymptotic (large T) forms. For $J \neq \frac{1}{4}$ they are

$$T^{+\frac{1}{2}\pm[\frac{1}{4}-J]^{\frac{1}{2}}}. \tag{3.1}$$

For $J = \frac{1}{4}$ these are degenerate and must be supplemented by

$$T^{\frac{1}{2}}\ln T. \tag{3.2}$$

The spatially averaged kinetic energy density per unit mass of a particular Fourier component is given by

$$2\bar{e} = \overline{\zeta\psi} \propto T^{-1\pm 2[\frac{1}{4}-J]^{\frac{1}{2}}}, \tag{3.3}$$

so that this simple model is stable to plane wave perturbations of all wave vectors for $J \geqslant 0$. This is in accord with similar models due to Taylor (1931) and Case (1960). For $J < 0$ the model under consideration is seen to exhibit no exponential instabilities, but only power-law instabilities, a characteristic feature of infinite Couette profiles.

A linearly independent pair of solutions to (2.11) is

$$\left.\begin{aligned} &(1+T^2)^{-\frac{1}{2}\mu}F(\tfrac{1}{2}\mu, \tfrac{1}{2}\mu+1;\, \mu+\tfrac{3}{2};\, (1+T^2)^{-1}),\\ &(1+T^2)^{\frac{1}{2}(\mu+1)}F(-\tfrac{1}{2}-\tfrac{1}{2}\mu, \tfrac{1}{2}-\tfrac{1}{2}\mu;\, \tfrac{1}{2}-\mu;\, (1+T^2)^{-1}),\end{aligned}\right\} \tag{3.4}$$

where

$$\mu = -\tfrac{1}{2}+[\tfrac{1}{4}-J]^{\frac{1}{2}} \tag{3.5}$$

and F is the standard Gauss hypergeometric function.† The pair (3.4) is useful because each is readily seen to be the complex conjugate of the other and they hence

† Another, more familiar, pair of solutions is $\phi^{-1}P'_\mu(\phi)$ and $\phi^{-1}Q'_\mu(\phi)$, where $\phi = (1+T^2)^{-1}$ and P_μ and Q_μ are the familiar Legendre functions. These are, however, not complex conjugates of each other and are not appropriate for our discussion. Here and throughout, we use the notation of Abramowitz & Stegun (1970), to which we refer as HMF followed by a section number.

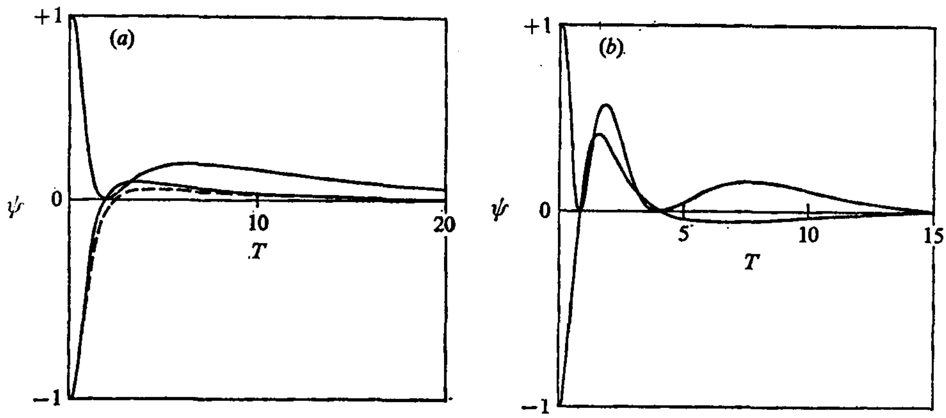

FIGURE 1. The exact (lower solid curve) and approximate (broken curve) stream functions for initial conditions $\psi(T = 0) = -1$, $d\psi/dT|_{T=0} = 0$. (*a*) $J = 1$. (*b*) $J = 5$. For $J = 5$ the approximate and exact solutions effectively coincide. The upper solid curve is the exact kinetic energy density $\propto \overline{\psi\zeta}$ but normalized to unity at $T = 0$.

will correspond naturally to travelling wave solutions. The hypergeometric series defining (3.4) are also evidently convergent for all T.

Values of J in the range $0 < J < \frac{1}{4}$ correspond to potentially unstable configurations in more realistic models, and although the behaviour of localized disturbances in the present model for this range of J is readily determined (Hartman 1973), we omit it here.

The range $J > \frac{1}{4}$ is characterized by the oscillatory behaviour of the asymptotic solutions [see (3.1)]. Throughout this region, then, the individual Fourier components will represent simple travelling waves in convected co-ordinates, and we may resort to the usual wave-packet dynamics to study the propagation and distortion of an initial wave-packet disturbance.

To facilitate the study of packet propagation, we first consider the exact solutions (3.4) in two limits. In the range $|J| \gg 1$ we may use an asymptotic form of the hypergeometric function due to Watson (Erdélyi *et al.* 1953, p. 77). In this limit we may write the solutions (3.4) in the form

$$(1+T^2)^{\frac{1}{4}}\,[T+(1+T^2)^{\frac{1}{2}}]^{\pm iJ^{\frac{1}{2}}}\,[1+O(J^{-\frac{1}{2}})]. \tag{3.6}$$

The usefulness of the pair (3.4) in studying travelling waves is now evident. For J positive, these solutions represent slowly growing vorticity oscillations of instantaneous frequency $RJ^{\frac{1}{2}}/(1+T^2)^{\frac{1}{2}}$. The algebraic (as opposed to exponential) growth for J negative is also evident from these solutions.

We comment in passing that the approximate solution (3.6) is a remarkably good representation of the exact solution even in the region $J \gtrsim 1$, as the comparisons in figure 1 indicate. This fortuitous circumstance will be of value in the next section when we discuss the behaviour of wave packets in this flow. It should be noted, and is easily verified from (3.6), that the oscillatory behaviour expected for $J > \frac{1}{4}$ is in fact quite poorly defined for $J \sim 1$ (see also figure 1).

The analyticity of the solutions (3.4) as functions of μ (Erdélyi *et al.* 1953, p. 68) may be used to obtain limiting forms of the solutions to (2.11) in the region $J \gtrsim \frac{1}{4}$. To accomplish this, we define ϵ through

$$\mu = -\tfrac{1}{2}+i\epsilon, \quad 0 \leqslant \epsilon \ll 1, \tag{3.7}$$

from which we see that

$$J = \tfrac{1}{4}+\epsilon^2. \tag{3.8}$$

We now wish to obtain the first term in a power series in ϵ for the solutions (3.4). We must supplement the set (3.4) with additional solutions valid at $\epsilon = 0$ (the set (3.4) is degenerate there). We choose as our fundamental set valid at $\epsilon = 0$ (Erdélyi *et al.* 1953, p. 75)

$$F_0(T) \equiv (1+T^2)^{\frac{1}{4}}\, F(-\tfrac{1}{4},\tfrac{3}{4};\, 1;\, (1+T^2)^{-1}), \tag{3.9a}$$

$$\tilde{F}_0(T) \equiv (1+T^2)^{\frac{1}{4}}\, F(-\tfrac{1}{4},\tfrac{3}{4};\, \tfrac{1}{2};\, T^2(1+T^2)^{-1}), \tag{3.9b}$$

and we write for convenience the solutions (3.4) near $\epsilon = 0$ as

$$F_{\pm}(\epsilon, T) \equiv (1+T^2)^{\frac{1}{4}\mp\frac{1}{2}i\epsilon}\, F(-\tfrac{1}{4}\pm\tfrac{1}{2}i\epsilon, \tfrac{3}{4}\pm\tfrac{1}{2}i\epsilon;\, 1\pm i\epsilon;\, (1+T^2)^{-1}). \tag{3.10}$$

A slightly involved but straightforward computation yields, to first order in ϵ,

$$F_{\pm}(\epsilon, T) = F_0(T) \pm i\epsilon[b_1 F_0(T) + b_2 \tilde{F}_0(T)] + O(\epsilon^2), \tag{3.11}$$

where b_1 and b_2 are explicit transcendental numbers: $b_1 \sim -1{\cdot}5$ and $b_2 \sim 2{\cdot}4$. Of primary interest to us is the phase of (3.11), so we write

$$F_{\pm}(\epsilon, T) \propto F_0(T)\, e^{\pm i\beta(T)}, \tag{3.12}$$

where

$$\beta(T) \cong b_2[J-\tfrac{1}{4}]^{\frac{1}{2}}\, \tilde{F}_0(T)/F_0(T) \tag{3.13}$$

and we have used the smallness of ϵ to write $\tan\epsilon \sim \epsilon$. Both $F_0(T)$ and $\tilde{F}_0(T)$ are easily shown to be monotonic functions of T and in particular it is a simple exercise to demonstrate that $F_0(T)$ has no zeros for real $T > 0$ and hence the phase (3.13) is well defined and finite for all $T > 0$, to which we restrict ourselves for simplicity.

We emphasize at this point that the solutions (3.4) provide, along with the Fourier inversion integral (2.13), the mathematically complete solution to the posed linear initial-value problem.

4. Wave-packet propagation

We now proceed to a discussion of the time evolution of initial wave-packet disturbances which are coherent superpositions of Fourier components with spread $\Delta\mathbf{k}$ about a central wave vector $\mathbf{k}_0$ subject to $|\Delta\mathbf{k}|/k_0 \ll 1$.† We shall limit our treatment, for the most part, to a discussion of the trajectory of the packet centre. The limitations of this wave-packet procedure due to packet dispersion are dealt with in the appendix. It is demonstrated there that, for $J \gg 1$, wave-packet dispersion (in convected co-ordinates) is pronounced, as it is in the zero-shear ($J = \infty$) situation, but does not alter the usefulness of the 'centre trajectory' analysis in either case. Somewhat surprisingly, packet dispersion becomes steadily

† Recall that the characteristic dimension L of a packet disturbance is given by $L \sim 1/|\Delta\mathbf{k}|$.

less significant as J decreases, until, at the lower limit of interest, $J = \frac{1}{4}$, dispersive effects disappear entirely with the vanishing of the group velocity. The dispersion in convected co-ordinates must not be confused with the unrelated *kinematic* dispersion evident in laboratory co-ordinates, which is a consequence of the mean shear. These kinematic effects have been eliminated by the transformation (2.7), allowing a closer scrutiny of the underlying dynamics (see figure 2).

The nonlinear development of our wave-packet disturbances has been considered (Hartman 1973) and does not contribute in any significant way to their evolution in this basic flow.

For $0 < J \leqslant \frac{1}{4}$ the solutions to (2.11) are purely monotonic, and hence wave packets in this domain will be subject only to minor distortion (in convected co-ordinates) as they surrender their energy (in a time $\sim 1/R$) to the mean flow at the level of their creation. In *laboratory* co-ordinates these disturbances will be spread by the mean flow over horizontal distances in direct proportion to the time. It should be evident that, as these solutions contain no time-dependent phase, disturbances in this regime cannot act as sources for internal wave radiation. Their influence, for practical purposes, cannot be felt at levels above (or below) the extreme levels which completely contain the initial perturbation. This conclusion clearly holds for all perturbations in our linear treatment, and not just the wave packets of immediate interest.

Before proceeding to a discussion of the case $J > \frac{1}{4}$, which admits propagating disturbances, we pause to examine the physical picture in this range of J. In laboratory co-ordinates there is a clear distinction between $J \sim 1$ and $J \gg 1$, for in the latter case we expect wave disturbances (packets) to propagate locally with little concern for the weak shear. Indeed Bretherton (1966) has shown that the validity of a WKB-type approximation to the governing equation (2.6) for this problem hinges precisely on the requirement $J \gg 1$. Somewhat more physically, this restriction can be traced directly to the requirement that the packet shape (in *laboratory* co-ordinates) should remain essentially unaltered during a characteristic oscillation period. To see this we note only that requiring the variation in the mean flow velocity across the packet dimension $L \sim 1/|\Delta\mathbf{k}|$ to be much smaller than the characteristic local packet velocity N/k_0 leads to

$$R/|\Delta\mathbf{k}| \ll N/k_0, \tag{4.1}$$

or equivalently

$$k_0/|\Delta\mathbf{k}| \ll J^{\frac{1}{2}}. \tag{4.2}$$

No such restrictions on J are necessary in convected co-ordinates. Our solution to the initial-value problem, and in particular the wave-packet application, does *not* require that the time scale for alteration of the initial configuration ($t \sim 1/R$) be large compared with the internal wave period ($t \sim 2\pi/N$).

We note once again that, as viewed in the 'lab' by a real observer, all of these disturbances, regardless of the value of J, are subject to a kinematic horizontal dispersion which is directly proportional to the time, in addition to the 'dynamic' dispersion considered in the appendix. That the packet, viewed in the lab, appears to lose its spatial integrity owing to the mean shear bears no relevance to the fact that the perturbation remains spatially coherent for its entire lifetime and hence may be treated as a packet in the conventional sense, most conveniently in convected co-ordinates.

We now choose the initial conditions to generate a wave packet travelling in only one direction. For the remainder of our discussion we shall limit ourselves to upward-propagating packets, for which $-\frac{1}{2}\pi \leqslant \theta_{k_0} \leqslant \frac{1}{2}\pi$. This is conveniently done by choosing $\zeta(\tau = 0)$ and $\dot{\zeta}(\tau = 0)$ such that only one of the complex solutions (3.4) occurs in $\tilde{\zeta}(\mathbf{k}, \tau)$. To isolate the phase of the solution, we write

$$\tilde{\zeta}(\mathbf{k}, \tau) = \tilde{\zeta}(\mathbf{k}, \tau = 0) f_m(\tau, \mathbf{k}) \exp[i\gamma(\tau, \mathbf{k})], \tag{4.3}$$

where f_m and γ are both real. The instantaneous position and group velocity of an initial wave-packet disturbance with central wave vector $\mathbf{k}_0$ (centred about $\boldsymbol{\xi} = 0$ at $\tau = 0$ for convenience) are then given in the usual way (see appendix) by

$$\boldsymbol{\xi}(\tau) = -\nabla_k \gamma(\tau, \mathbf{k})|_{\mathbf{k}_0}, \tag{4.4}$$

$$\mathbf{v}_g(\tau) = [-\partial(\nabla_k \gamma(\tau, \mathbf{k}))/\partial\tau]_{\mathbf{k}_0}, \tag{4.5}$$

where ∇_k is the gradient operator in wave-vector space.

We are now in a position to calculate the motion of wave packets in the system at hand. Of particular interest is their *vertical* motion, since this feature of the calculation will not be affected by the transformation back to laboratory co-ordinates.

For $J > 1$ we use the approximate solutions (3.6), which, though derived for the limit $J \gg 1$, are expected to give reasonably reliable results for all $J > 1$ on the basis of figure 1. We find in this limit for an upward-propagating packet

$$\boldsymbol{\xi}(\tau) = -\frac{J^{\frac{1}{2}}}{k_0 \cos^2\theta_{k_0}} \left[\frac{1}{(1+T_0^2)^{\frac{1}{2}}} - \cos\theta_{k_0}\right] \hat{\boldsymbol{\theta}}_{k_0}. \tag{4.6}$$

Here (k_0, θ_{k_0}) represents the polar co-ordinate decomposition of $\mathbf{k}_0$. (See also footnote on p. 91.) The ultimate vertical displacement is then given by

$$z(\infty) = \hat{\mathbf{z}} \,.\, \boldsymbol{\xi}(\infty) = J^{\frac{1}{2}}/k_0. \tag{4.7}$$

This is the result, given by Bretherton (1966) for $J \gg 1$, that such wave packets are limited in their vertical motion by the 'critical level' $Z_c = N/Rk_0$ corresponding to their laboratory frequency $N(k_1/k)_0$. We see that in this context the result is expected to be valid for all J for which the approximate solution (3.6) is a reasonable representation of the exact solution (3.4) to the linear equations of motion.

In the range $J \gtrsim \frac{1}{4}$ we use the results of (3.11)–(3.13). We find in this limit

$$\boldsymbol{\xi}(\tau) = \frac{(J-\frac{1}{4})^{\frac{1}{2}}\alpha}{k_0 \cos^2\theta_{k_0}} \left[\frac{1}{F_0^2(T_0)}\bigg|_{\tau=0} - \frac{1}{F_0^2(T_0)}\right] \hat{\boldsymbol{\theta}}_{k_0}, \tag{4.8}$$

where $\alpha = b_2 W(\tilde{F}_0, F_0) \sim 1{\cdot}4$ and $W(\tilde{F}_0, F_0)$ is the (constant) Wronskian of the solutions $\tilde{F}_0$ and F_0. The function $F_0(T)$ is easily shown to lie in $C \leqslant F_0 < \infty$ for $0 \leqslant T < \infty$, where $C \sim 0{\cdot}5$. The ultimate vertical displacement of this packet is seen to be

$$z(\infty) = \frac{\alpha(J-\frac{1}{4})^{\frac{1}{2}}}{k_0 \cos\theta_{k_0}} \frac{1}{F_0^2(T_0)}\bigg|_{\tau=0}. \tag{4.9}$$

The factors occurring in (4.9) are all $O(1)$ (the product $F_0^2 \cos\theta_{k_0} \to$ constant as $\theta_{k_0} \to \frac{1}{2}\pi$) so the important feature of this exercise is that the packet centre moves vertically, in the limit $J \gtrsim \frac{1}{4}$, only a small fraction of its initial central wavelength, which is in turn a small fraction of its overall dimension. We expect this result to provide a rough approximation to the packet motion for $\frac{1}{4} < J \lesssim 1$, so that the result (4.9), along with (4.7), provides a fairly complete picture of the propagation of initial wave-packet disturbances throughout the physical range $\frac{1}{4} < J < \infty$.

From the results (4.7) and (4.9) it is apparent that a useful interpolation formula, giving the order of magnitude of the maximum vertical displacement of a wave-packet disturbance in a stratified shear flow, is

$$\Delta z \sim (J - \tfrac{1}{4})^{\frac{1}{2}}/k_0. \tag{4.10}$$

The final vertical distribution of the initial perturbation energy is now given in a straightforward way from the time dependence of the kinetic energy density $\overline{\psi\zeta}$ and (4.4). It is worthwhile to note that the energy density of these disturbances varies continuously on a time scale $t \sim 1/R$. This behaviour may be traced to the action of Reynolds stresses, working at the packet edges (and *not* throughout the volume) to transfer energy to and from the mean flow. For a detailed discussion see Booker & Bretherton (1967, § 6). For $J \gg 1$, it may be trivially verified from (3.6) that *maximum* energy transfer occurs at $|T_0| = 2^{-\frac{1}{2}}$. In terms of the packet's vertical position, this corresponds to only $\sim 20\,\%$ of the ultimate vertical displacement of a packet with an initially horizontal wave vector. Similar observations for the case $J \gtrsim \frac{1}{4}$ also apply.

For reasons that will become apparent shortly, we designate that level in the flow which corresponds to the ultimate vertical displacement of a wave packet's centre (e.g. (4.7) or (4.9)] as its *isolation level* Z_I.

The basic physical results of this section are summarized in figure 2 for a specific initial disturbance. We have chosen $J \gg 1$ to facilitate the visual presentation.

In convected co-ordinates. (i) The total packet displacement, for the choice of parameters in figure 2, is of the order of several packet diameters. (ii) The motion is rectilinear [see (4.6)] and, with the neglect of dispersive effects, the packet envelope is not altered in time. [The dispersive effects, as given in the appendix, would give rise in the limit $t \to \infty$ to a distortion and growth of the envelope of order $10\,\%$ (see (A 5)).] (iii) The packet's central wave vector $\mathbf{k}_0$, as mentioned earlier, remains constant in time (see footnote on p. 91).

In laboratory co-ordinates. (i) The horizontal packet motion is unlimited, the original disturbance eventually being swept to infinity by the mean flow. (ii) The vertical motion of the packet centre, as in convected co-ordinates, is confined below the isolation level Z_I, but approaches it as $t \to \infty$. (iii) The packet envelope is distorted in time into an eccentric ellipse whose major and minor axes, for large t, are of order LRt and $L/(Rt)$ respectively. (iv) The central wave vector $\boldsymbol{\kappa}_0(t)$ rotates towards the vertical and ultimately increases in magnitude in proportion to $(Rt)^2$ (see footnote on p. 91). (v) The position and velocity of the packet centre are given (for any value of J), from (4.4) and (2.7), by

$$z(t) = \eta(t), \quad x(t) = \xi(t) + R\eta(t)\,t, \tag{4.11a,b}$$

$$v_z(t) = dz(t)/dt, \quad v_x(t) = dx(t)/dt. \tag{4.12a,b}$$

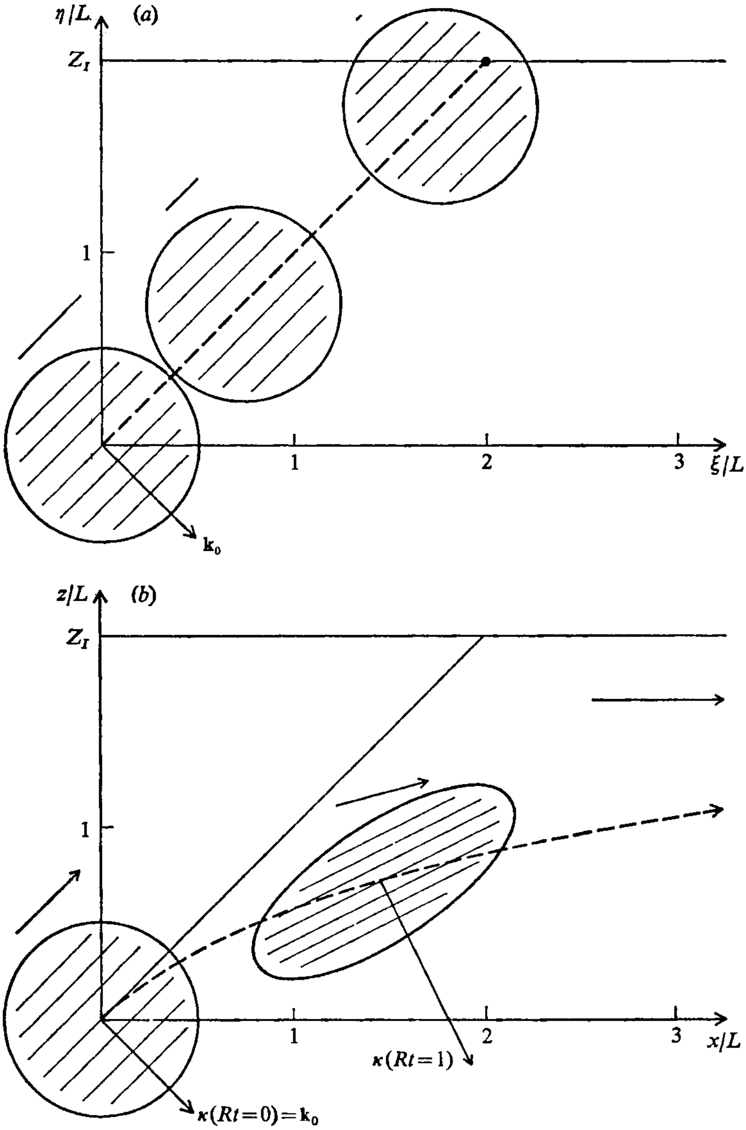

FIGURE 2. The development of an initially circular wave packet of diameter $L \sim 4{\cdot}2\lambda$ ($\lambda \equiv 2\pi/k_0$) in (*a*) convected and (*b*) laboratory co-ordinates. $J \sim 2800$, $\theta_{k_0} = -\frac{1}{4}\pi$. The isolation level is $Z_I = 2L$. Three successive instants, $Rt = 0$, 1 and 10, are depicted. Lines within the packet envelope represent points whose motions are 180° out of phase. Dispersive modifications (see appendix), amounting to at most 10 %, have been neglected. In (*a*) lines above and to the left of each packet represent the magnitude of (4.5); the large terminal dot represents the limiting ($t \to \infty$) position of the packet centre. In (*b*) the arrows above the figures represent the velocity of the packet centre; the highly eccentric packet corresponding to $Rt = 10$ is off the figure, with centre at $(x, z) \sim (20L,\ 1{\cdot}8L)$, length $\sim 10L$ and thickness $\sim \frac{1}{10}L$. The horizontal arrow in (*b*) represents the ultimate velocity $\mathbf{v} = RZ_I\hat{\mathbf{x}}$ of the packet centre.

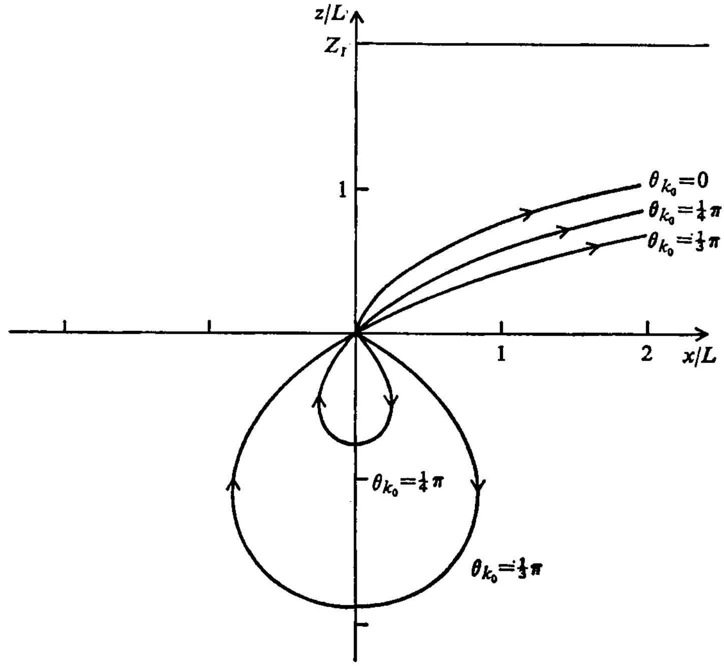

FIGURE 3. Packet-centre trajectories, in laboratory co-ordinates, for the parameters of figure 2. The initial wave-vector magnitude k_0 is the same for each trajectory and the polar angles θ_{k_0} are given on the figure. For $\theta_{k_0} = -\frac{1}{4}\pi, -\frac{1}{3}\pi$ the trajectories are identical to the $z > 0$ portion of those for $\theta_{k_0} = \frac{1}{4}\pi, \frac{1}{3}\pi$ respectively (compare figure 2). The bottom of the loop is reached at $Rt = \tan\theta_{k_0}$ ($T_0 = 0$), and the packet centre returns to the origin at $Rt = 2\tan\theta_{k_0}$.

Notice that the packet's horizontal velocity in laboratory co-ordinates (4.12*b*) is *not* simply the sum of the $\hat{\xi}$ component (4.5) of the group velocity in convected co-ordinates and the local convection speed $R\eta(t)$ as might be anticipated. This is due to the non-orthogonality (in laboratory co-ordinates) of the surfaces of constant ξ and η.

In figure 3 we have displayed several packet-centre trajectories for values of θ_{k_0} in the range $0 \leqslant \theta_{k_0} < \frac{1}{2}\pi$. This remarkable motion is accompanied by a growth in packet energy density to a maximum of $\sec\theta_{k_0}$ times the initial ($t = 0$) value [see (3.6)]. The extreme energy density occurs at $T_0 = 0$ ($Rt = \tan\theta_{k_0}$), which corresponds to the loop bottoms in figure 3. The width W and vertical extent Δ of the loops are given in a straightforward way by (4.11), (4.12) and (4.6):

$$W(\theta_{k_0}) = 2Z_I[\sec^{\frac{2}{3}}\theta_{k_0} - 1]^{\frac{3}{2}}, \quad \Delta(\theta_{k_0}) = Z_I[\sec\theta_{k_0} - 1].$$

As pointed out in the appendix, the wave-packet analysis fails for $\tan\theta_{k_0} \gtrsim (Lk_0)^{\frac{1}{2}}$ but can be expected to give qualitatively reliable results for $\tan\theta_{k_0} \lesssim (Lk_0)^{\frac{1}{2}}$ (quantitative reliability requires $\tan\theta_{k_0} \ll (Lk_0)^{\frac{1}{2}}$). As $\theta_{k_0} \to \tan^{-1}(Lk_0)^{\frac{1}{2}}$ we have to a good approximation $\Delta \sim Z_I(Lk_0)^{\frac{1}{2}}$ and $W \sim 2\Delta$, so that the loops become large in this limit. In particular they reach points in the flow which lie at distances considerably greater than the distance Z_I to the isolation level, but in the opposite direction. Characteristic trajectories of packets with $\frac{1}{2}\pi < \theta_{k_0} < \frac{3}{2}\pi$ may be obtained by reflecting figures 2 and 3 in both the x and z planes. Packets traversing the loops of figure 3 return to the origin in a time $Rt = 2\tan\theta_{k_0}$ with central wave vectors of magnitude $\kappa\,(Rt = 2\tan\theta_{k_0}) = k_0$ and envelopes distorted by the mean shear (see the subsequent discussion for details of the distortion process).

The regime $J \gtrsim \frac{1}{4}$ is characterized by the following features.

(i) A total vertical displacement (i.e. distance to the isolation level) whose magnitude is considerably less than a wavelength λ [see (4.10)].

(ii) The initial packet envelope, being large compared with λ, extends well beyond the packet's isolation level. (Recall from (4.11a) that all comments regarding the packet's *vertical* co-ordinate apply in both laboratory and convected co-ordinate systems.)

(iii) Viewed in laboratory co-ordinates, the disturbance never completely escapes from the region about $x = 0$ as it does for larger J (figure 2), for the group velocity, whose magnitude [from (4.5)] is of order $R(J-\frac{1}{4})^{\frac{1}{2}}/k_0$, is much smaller than the extreme convective speeds $\pm\frac{1}{2}RL$ of the packet envelope region. Hence, although the packet *centre* ultimately proceeds towards infinity at a velocity approaching $RZ_I\hat{\mathbf{x}}$, the envelope, which eventually encloses a thin, nearly horizontal fluid layer, always crosses $x = 0$ (it also always crosses $z = 0$ since $Z_I < L$). It should perhaps be pointed out that, neglecting dispersive effects, the development of the packet *envelope* is purely kinematic. The development may be regarded as the kinematic distortion of the initial envelope due to convection by the mean shear. Therefore, disregarding dispersion, Rt is a similarity parameter for packet envelopes in flows of differing J; the development of a packet envelope is independent of the packet's wave vector.

We conclude this section by emphasizing that the motion of wave-packet disturbances in these flows is characterized by a smooth, orderly, transition from large group velocities and vertical displacements for $J \gg 1$ to zero group velocity and vertical displacement for $J = \frac{1}{4}$.

5. A comparison with Booker & Bretherton

To make contact with the usual normal-mode treatments of this system, we begin by considering the normal-mode decomposition of an arbitrary wave packet of dimension L and initial central wave vector $\mathbf{k}_0$. A single normal-mode solution is

$$f_{k_1,\omega}(z)\exp\left[i(k_1x-\omega t)\right],$$

where $f(z)$ is determined from the normal-mode governing equation plus boundary conditions. The vertical structure of the packet is determined by that collection of modes associated with $k_1 = k_{10}$ and frequency spectrum characterizing the packet as a whole. (*Complete* specification of the packet would, roughly speaking, include for *each* horizontal wave vector $k_{10}-\Delta k_1 < k_1 < k_{10}+\Delta k_1$ a *set* of modes (k_1, ω) corresponding to that wave vector and the packet's frequency spectrum.) The frequency of motion at the packet *centre* is $\omega_0 = N(k_1/k_0)$, while the effect of the mean shear is to Doppler shift this central frequency to $\omega \sim \omega_0 \pm \frac{1}{2}RLk_{10}$ at the upper and lower packet extremes. (Note that this entire discussion is relevant only to the laboratory co-ordinate system.) This characteristic set of frequencies remains unchanged as time passes (only in the convected system is the packet frequency time dependent). Notice that

$$\Delta\omega/\omega_0 = J^{-\frac{1}{2}}Lk_0, \tag{5.1}$$

where $\Delta\omega$ is the frequency spread RLk_{10}, so that only when

$$J^{\frac{1}{2}} \gg Lk_0 \tag{5.2}$$

can we sensibly speak of a single packet frequency ω_0. Recall that this important condition has already appeared, in a slightly different context, in § 4, equation (4.2).

Only if (5.2) is satisfied will the normal-mode decomposition of a wave packet be dominated by the single normal mode corresponding to (k_{10}, ω_0) (which we identify hereafter as 'the central normal mode'). In that case we certainly expect the normal-mode critical-level discontinuity $\exp\{-\pi(J-\frac{1}{4})^{\frac{1}{2}}\}$ of Booker & Bretherton to play an important role in packet development, and in (4.7) it was shown that, in fact, the packet isolation level Z_I is identical to the critical level Z_c of the central normal mode in this range of J.

In view of (5.1) and the fact that Lk_0 can be made arbitrarily large in this discussion, there exists a substantial range of $J \gg 1$ for which $\Delta\omega/\omega_0$ is *not* small and for which the normal-mode decomposition of a packet disturbance is, therefore, not dominated by the central mode. In this range ($J \gg 1$ but $J < (Lk_0)^2$) we should not necessarily expect coincidence between the isolation level and the critical level of the central mode. It is rather remarkable that, according to (4.7), these levels actually coincide for *all* $J \gg 1$ (and very nearly coincide even for $J \gtrsim 1$). For $\frac{1}{4} \leqslant J < 1$ this somewhat surprising correlation finally breaks down with $Z_I \sim (J-\frac{1}{4})^{\frac{1}{2}}/k_0$ and $Z_c = J^{\frac{1}{2}}/k_0$. In this latter regime Z_I and Z_c both remain well within the packet envelope for all time, both being, in fact, smaller than a wavelength.

It remains to reconcile the essentially non-existent wave-packet propagation in the regime $J \gtrsim \frac{1}{4}$ with the large (nearly unit) critical-level 'transmission coefficient' of Booker & Bretherton. As we have seen, a wave packet is necessarily associated with a spectrum of frequencies within $\pm\frac{1}{2}Rk_{10}L$ of its central frequency $\omega_0 = N(k_1/k)_0$. For $J \sim \frac{1}{4}$ we have $R \sim 2N$, so that

$$-Lk_0\omega_0 < \omega < Lk_0\omega_0 \tag{5.3}$$

roughly defines the relevant spectrum of normal-mode frequencies. Now $\Delta\omega/\omega_0 \sim Lk_0 \gg 1$, so (5.3) shows that there is essentially an equal number of positive- and negative-frequency normal modes. Since the sign of the frequency of a mode (for $k_1 \sim k_{10}$) corresponds to the direction of its individual contribution to the momentum flux (i.e. to the sign of both horizontal *and* vertical components), the net momentum flux of the superposition of modes may be (and is) arbitrarily small. The marked reduction in net momentum flux due to this cancellation is further enhanced by the relative weakness of the Reynolds stresses in this regime (these go like $(J-\frac{1}{4})^{\frac{1}{2}}$; see Booker & Bretherton 1967).

It should be emphasized here that (i) the substantial cancellation of normal-mode momentum flux, (ii) the large relative frequency spread $\Delta\omega/\omega_0$ and (iii) the perpetual intersection of the lines $x = 0$ and $z = 0$ by the packet envelope (see § 4) are but a few of a large class of equivalent statements applying to the *entire* range $\frac{1}{4} \leqslant J < (Lk_0)^2$. In this range, we must, from the normal-mode point of view, use normal modes with critical levels on both sides of $z = 0$ to construct a packet, and we should not expect that any single mode in that collection (e.g. the 'central' mode) would reflect in an accurate way the development of the wave group as a whole. Again, it must be viewed as accidental that such a procedure actually leads to a qualitatively accurate picture of wave propagation in these flows in the range $1 < J < (Lk_0)^2$.

In summary, the normal-mode approach is, as it must be, entirely compatible with our treatment. The discussion here does, however, point out the care with which the analysis of wave propagation based on the consideration of single normal modes must be made.

6. Conclusions and discussion

We have presented an alternative to the initial-value problem of Eliassen *et al.* and of Case for an unbounded fluid which is sufficiently tractable analytically to consider the evolution of initial perturbations of physical interest.

In calculating the detailed trajectories of wave-packet disturbances to the basic flow (2.1), we find that the rather intricate possible motions share one important common feature: the existence of an 'isolation level' in the flow beyond which the packet centre cannot penetrate. For a packet originally at $z = 0$, the magnitude of this ultimate vertical co-ordinate is $|Z_I| \sim (J-\frac{1}{4})^{\frac{1}{2}}/k_0$ for all $J \geqslant \frac{1}{4}$. In terms of overall packet motion, the vigour and extent of that motion is a smoothly varying function of the Richardson number J, and vanishes in a uniform manner as $J \to \frac{1}{4}$. Thus the vertical transport of energy and momentum for this class of disturbances also vanishes in a regular way as $J \to \frac{1}{4}$.

Of the semi-infinite range of J for which our model is stable, three subranges are of physical significance.

(i) For $0 \leqslant J \leqslant \frac{1}{4}$ no propagation occurs and localized disturbances are absorbed into the mean flow at the level of their creation.

(ii) For $\frac{1}{4} \leqslant J \lesssim (Lk_0)^2$, the packet's isolation level lies within the packet dimension L and wave-packet envelopes never completely escape the vicinity ($x = z = 0$) of their creation, although their centres do eventually propagate towards infinity at the speed $\mathbf{v} = RZ_I\hat{\mathbf{x}}$.

(iii) For $(Lk_0)^2 < J < \infty$ packets do escape from the origin (in the sense that the packet envelope eventually fails to intercept either the x or z axis).

These three divisions also arise naturally in a careful normal-mode treatment of wave-packet propagation.

In reconciling our results with the normal-mode approach of Booker & Bretherton (1967), we have seen that for $J \gg (Lk_0)^2$ the results of a rigorous wave-packet treatment are entirely compatible with the interpretation of the squared normal-mode critical-level discontinuity $\exp\{-2\pi(J-\frac{1}{4})^{\frac{1}{2}}\}$ as a 'transmission coefficient' for realistic wave disturbances. For $J \gtrsim 1$ the critical-level discontinuity, considered as a transmission coefficient, leads to essentially correct conclusions regarding wave propagation, although this circumstance must be viewed as largely accidental in view of the discussion in § 5. In the regime $\frac{1}{4} < J < 1$, the consideration of a *single* normal mode fails utterly to provide a realistic physical description of the localized disturbances of the kind considered here, and a proper superposition of modes is essential to an understanding of wave phenomena in this range of J. It is unfortunate, in a way, that one *can* correctly infer a great deal about the development of wave disturbances in the range $1 \leqslant J < (Lk_0)^2$ by considering an isolated normal mode, for such a procedure must surely fail in general. Only when a wave group can sensibly be associated with a single frequency (e.g. when $J > (Lk_0)^2$), and hence is dominated by a normal mode associated with that frequency, may one anticipate a strong correspondence between the development of the wave group and the properties of the associated normal mode.

This research was supported by the National Science Foundation Grant GP-34637X and the Advanced Research Projects Agency of the Department of Defense Grant DA-ARO-D-31-124-72-G181.

Appendix. Packet propagation, modification and dispersion

We refer to any good electrodynamics or acoustics textbook (e.g. Stratton 1941, chap. 9) for a thorough discussion of wave-packet dynamics. For our purposes we summarize below the results of applying the wave-packet procedure to the initial disturbance (A 1) [and associated Fourier transform (A 2)]. We have

$$\zeta(\mathbf{x}, t = 0) = \zeta(\boldsymbol{\xi}, \tau = 0) = a(\boldsymbol{\xi}) \exp[i\mathbf{k}_0 . \boldsymbol{\xi}], \qquad (\text{A } 1)$$

$$\tilde{\zeta}(\mathbf{k}, t = 0) = \tilde{a}(\mathbf{k} - \mathbf{k}_0) \equiv \tilde{a}(\delta\mathbf{k}). \qquad (\text{A } 2)$$

Here $a(\boldsymbol{\xi})$ is the packet 'envelope' function of typical dimension L. Expanding to first order in $(Lk_0)^{-1}$ in the integrand of (2.13) we find

$$\zeta(\boldsymbol{\xi}, \tau) = a(\boldsymbol{\xi} + \nabla_k \gamma(\mathbf{k}, \tau)) f_m(\mathbf{k}_0, \tau) \exp\{i[\gamma(\mathbf{k}_0, \tau) + \mathbf{k}_0 . \boldsymbol{\xi}]\}. \qquad (\text{A } 3)$$

From (A 3) the results (4.4) and (4.5) follow directly. Here $f_m(\mathbf{k}_0, \tau)$ occurs as a simple time-dependent packet amplitude. To study packet dispersion and shape modification, we must consider corrections of order $(Lk_0)^{-2}$ in the expansions leading to (A 3). At this order, f_m preferentially alters the amplitudes of the various Fourier components occurring in (2.13) and thus gives rise to packet shape modifications. These modifications are small and uninteresting and can be dealt with in a straightforward manner (Hartman 1973). We ignore them entirely in this presentation.

The phase $\gamma(\mathbf{k}, \tau)$ determines the interesting features of packet propagation (A 3) and dispersion. Rather than outline a rigorous mathematical treatment of dispersion in this system, we resort to physical arguments for brevity. The dispersion of the packet is due to a spread in the group velocity $\Delta\mathbf{v}_g$ arising from the spread in wave vectors $|\Delta\mathbf{k}| \sim 1/L$. The effect on the overall packet size and shape due to the dispersion is measured by $\Delta L(\tau)/L$, where

$$\Delta L(\tau) \equiv \int_0^\tau \frac{1}{L}\,|\nabla_k v_g(\mathbf{k},\tau')|_{\mathbf{k}_0}\,d\tau'. \tag{A 4}$$

Here the integrand is an appropriate measure of the instantaneous spread in group velocity. From (4.4), (4.5), (4.10) and (A 4) we can write, for the maximum packet distortion,

$$\frac{\Delta L(\infty)}{L} \sim \frac{1}{L^2}\frac{\partial|\xi(\infty)|}{\partial k_0} \sim \frac{(J-\frac{1}{4})^{\frac{1}{2}}}{(Lk_0)^2}. \tag{A 5}$$

Physically, the dispersion for $J \sim 1$ is limited because of the reduced time scale $1/R$ for the dispersive effects to occur. In the weak-shear limit $J \gg (k_0 L)^2$ the packet dispersion approaches that for the zero-shear (or acoustic, or electromagnetic) case, in which the packet always eventually spreads in proportion to the time (in a dispersive medium).

Hence, somewhat paradoxically, the packet *size* in convected co-ordinates is much less affected during its lifetime for $J \sim 1$ than for $J \gg 1$. That is to say our concepts of packet 'centre' and 'edges' are more valuable and more precisely definable in the small-J case than for $J \gg 1$, where wave-packet approaches have previously been used (Bretherton 1966).

As a final caveat, we point out the limitations of the wave-packet analysis imposed by the expansion leading to (A 3). For $\tan\theta_{k_0} > 0$ the procedure leading to (A 3) requires

$$\tan\theta_{k_0} \ll (Lk_0)^{\frac{1}{2}}, \tag{A 6}$$

while for $\tan\theta_{k_0} < 0$, we must have

$$|\tan\theta_{k_0}| \ll Lk_0. \tag{A 7}$$

Thus the analysis fails for packets whose initial central wave vectors lie sufficiently close to the vertical. Qualitatively, however, we can expect the analysis of § 4 to be useful throughout the range

$$0 \leqslant \tan\theta_{k_0} \lesssim (Lk_0)^{\frac{1}{2}}, \quad -Lk_0 \lesssim \tan\theta_{k_0} \leqslant 0.$$

REFERENCES

ABRAMOWITZ, M. & STEGUN, I. 1970 *Handbook of Mathematical Functions.* Washington: Nat. Bur. Stand.

BOOKER, J. R. & BRETHERTON, F. P. 1967 *J. Fluid Mech.* **28**, 545.

BRETHERTON, F. P. 1966 *Quart. J. Roy. Met. Soc.* **95**, 213.

CASE, K. M. 1960 *Phys. Fluids*, **3**, 149.

DYSON, F. J. 1960 *Phys. Fluids*, **3**, 155.

ELIASSEN, A., HØILAND, E. & RIIS, E. 1953 *Two-Dimensional Perturbation of a Flow with Constant Shear of a Stratified Fluid.* Inst. for Weather & Climate Res., Norwegian Acad. Sci. & Lett., publ. no. 1.

ERDÉLYI, A., MAGNUS, W., OBERHETTINGER, F. & TRICOMI, F. G. 1953 *Higher Transcendental Functions*, vol. 1. McGraw-Hill.

HARTMAN, R. J. 1973 Ph.D. dissertation, University of California, Santa Barbara.

HAZEL, P. 1967 *J. Fluid Mech.* **30**, 775.

PHILLIPS, O. M. 1966 *The Dynamics of the Upper Ocean.* Cambridge University Press.

STRATTON, J. A. 1941 *Electromagnetic Theory.* McGraw-Hill.

TAYLOR, G. I. 1931 *Proc. Roy. Soc.* A **132**, 499.